



HAL
open science

Three-dimensional treatment of nonequilibrium dynamics and higher order elasticity

Martin Lott, Cédric Payan, Vincent Garnier, Quang Vu, Jesús Eiras, Marcel Remillieux, Pierre-Yves Le Bas, T.J. Ulrich

► **To cite this version:**

Martin Lott, Cédric Payan, Vincent Garnier, Quang Vu, Jesús Eiras, et al.. Three-dimensional treatment of nonequilibrium dynamics and higher order elasticity. *Applied Physics Letters*, 2016, 108 (14), pp.14190. 10.1063/1.4945680 . hal-01299572

HAL Id: hal-01299572

<https://hal.science/hal-01299572>

Submitted on 20 May 2024

HAL is a multi-disciplinary open access archive for the deposit and dissemination of scientific research documents, whether they are published or not. The documents may come from teaching and research institutions in France or abroad, or from public or private research centers.

L'archive ouverte pluridisciplinaire **HAL**, est destinée au dépôt et à la diffusion de documents scientifiques de niveau recherche, publiés ou non, émanant des établissements d'enseignement et de recherche français ou étrangers, des laboratoires publics ou privés.

Copyright

Three-dimensional treatment of nonequilibrium dynamics and higher order elasticity

Martin Lott,^{1,a)} Cédric Payan,¹ Vincent Garnier,¹ Quang A. Vu,¹ Jesús N. Eiras,² Marcel C. Remillieux,³ Pierre-Yves Le Bas,³ and T. J. Ulrich³

¹LMA, Aix-Marseille Université, CNRS, UPR 7051, Centrale Marseille, 13453 Marseille Cedex 13, France

²Instituto de Ciencia y Tecnología del Hormigón ICITECH; Universitat Politècnica de València, Camino de Vera s/n, 46022 València, Spain

³Geophysics Group (EES-17), Los Alamos National Laboratory, Los Alamos, New Mexico 87545, USA

(Received 30 January 2016; accepted 26 March 2016; published online 6 April 2016)

This letter presents a three-dimensional model to describe the complex behavior of nonlinear mesoscopic elastic materials such as rocks and concrete. Assuming isotropy and geometric contraction of principal stress axes under dynamic loading, the expression of elastic wave velocity is derived, based on the second-order elastic constants (λ, μ), third-order elastic constants (l, m, n), and a parameter α of nonclassical nonlinear elasticity resulting from conditioning. We demonstrate that both softening and recovering of the elastic properties under dynamic loading is an isotropic effect related to the strain tensor. The measurement of the conditioning is achieved using three polarized waves. The model allows the evaluation of the third-order elastic constants uncoupled from conditioning and viscoelastic effects. The values obtained are similar to those reported in the literature using quasi-static loading. © 2016 AIP Publishing LLC. [<http://dx.doi.org/10.1063/1.4945680>]

In 1937, Murnaghan¹ proposed a general tensorial description of the nonlinear stress-strain relationship in the elastic isotropic materials. The constitutive relation of the materials was derived from the elastic energy and expressed in terms of the invariants of the Lagrangian finite strain tensor. Hughes and Kelly² simplified Murnaghan's theory by considering the particular case of acousto-elasticity experiments, where a pulse of relatively small amplitude (probe) is used to probe the local change of elastic wave speed induced by a large deformation (pump). In these conditions, it is possible to define the Lagrangian strain tensor in terms of small perturbations and use an infinitesimal strain superimposed to a triaxial finite strain. It follows then that the elastic wave velocities can be expressed as a function of the applied static stress through the coupling with the triaxial finite strain, using the third order elastic constants (l, m, n) in the elastic tensor. Since the 1970s, the experimental determination of the third order elastic constants under static loading conditions has been successfully conducted for a number of applications, including the quantification of residual stresses in solids.^{3,4} Various authors have also reported the complex nonlinear behavior of rocks and concrete under dynamic solicitation.⁵ In addition to the classical nonlinearity described by third-order elastic constants, they also reported nonclassical nonlinearity, including the presence of hysteresis with end-point memory in the stress-strain relationship, phase shifts in resonance experiments, amplitude-dependent attenuation, and conditioning.^{6,7} Conditioning refers to the softening of the material when dynamically loaded. Such behavior cannot be explained by Murnaghan's theory. McCall and Guyer^{8,9} and Johnson and Sutin¹⁰ separated the effects. A one-dimensional equation of state ($\sigma = K(1 + \beta\epsilon + \delta\epsilon^2)\epsilon + \gamma[\epsilon, \dot{\epsilon}]$) was proposed to combine classical (β, δ)

and nonclassical (γ) contributions in the description of the nonlinear elasticity. Recently, Renaud *et al.*^{6,7} developed an experimental methodology termed Dynamic Acousto-Elastic Testing (DAET) to obtain the nonlinear parameters of solids under dynamic loading, using the one-dimensional equation of state proposed in Ref. 8. It is shown that the parameters quantifying classical nonlinearity are strain dependent. However, using the one-dimensional equation of state, the strain induced anisotropy described by Hughes and Kelly² is neglected. Nonlinear anisotropic effects are also reported in unconsolidated granular media (e.g., packed glass beads)¹¹ during dynamic solicitation, where Hertzian contacts occur when the strain reaches a sufficiently large amplitude. The resulting nonlinear behavior is anisotropic and probed with different polarized waves. However, the equation of state proposed for unconsolidated granular media is not applicable to nonlinear mesoscopic elastic materials since it is limited to one scale (i.e., all beads have the same size) and nonlinearity is only governed by the Hertzian contacts between the beads.

The aim of this paper is to combine Murnaghan's theory with a tensorial formulation of nonequilibrium dynamics. The study describes how conditioning is introduced in the elastic tensor and its influence on the elastic wave velocities. The model is validated using DAET experiments. In these experiments, the sample is probed with three polarized pulses (probe with low strain) while it is excited in a longitudinal mode of vibration (pump with large strain).

The influence of conditioning appears in the elastic bulk modulus K .⁸⁻¹⁰ This effect implies that the local elastic energy of the solid body is not a constant. It is temporarily converted into nanoscale *potential* energy which does not contribute to the elasticity any more.¹²⁻¹⁴ The origins of these effects occur at the microstructural scale within microcracks and grain boundaries.^{8,15} Mortar is an amorphous

^{a)}lott@lma.cnrs-mrs.fr

medium essentially made of sands and cement paste. The contact zones appear at grain boundaries. Microstructural scales of mortar range from μm for cement paste to hundreds of μm for sand. The length scale of contacts should then be smaller, ranging from nm to μm . At a macroscopic scale, the loss and recovery of elastic energy observed in acoustic experiments is well described by thermodynamic process. In this process, a volume with a given density of discrete unformed bonds is represented as a smooth spectrum of energy barriers.^{12,16} A uniform distribution of nonlinear sources implies an isotropic effect on the elastic response. Under those assumptions, a three-dimensional tensorial strain field defined by six components (the most general case) is considered. The symmetric property of the strain tensor implies the existence of principal stress axes through its diagonalization: locally, the strain effect may always be seen as “compressive.” To quantify the influence of conditioning, the stress/strain relationship is written on the principal strain directions with contracted axes. The tensorial product between the strain and stress vector bases δ_{ij} is the natural basis for the elastic tensor and should now include the conditioning. With n_i as a principal strain direction, the conditioning is a scalar quantity α and $\Delta\epsilon_i$ is the strain amplitude in a basis formed by its principal axes. The new product

$$\delta_{ij} = n_i^{\text{Stress}} \otimes n_j^{\text{Strain}} \rightarrow \delta_{ij}(1 - \alpha(\Delta\epsilon_i)) = \Lambda_{ij}, \quad (1)$$

may explain the influence of conditioning on the 1st order elastic tensor. It means that an anisotropy induced by conditioning is actually an isotropic effect relative to the strain tensor on its principal axes. In case of textured media with oriented micro-cracks, those assumptions may not be valid anymore in the sense that α may no longer be a scalar.

Hughes and Kelly² formulated the elastic isotropic media with classical nonlinearity under loading as

$$\begin{aligned} C_{ijkl} = & \left[\lambda + 2(l - \lambda - m)Tr(\underline{\epsilon}) + 2(\lambda + m)(\epsilon_i + \epsilon_k) - 2\mu\epsilon_i \right] \\ & \times (\delta_{ij}\delta_{kl}) + [\mu + (\lambda + m - \mu)Tr(\underline{\epsilon}) + 2\mu(\epsilon_i + \epsilon_j + \epsilon_l)] \\ & \times (\delta_{ik}\delta_{jl} + \delta_{il}\delta_{jk}) + \frac{1}{2}n \sum_v (\delta_{jvk}^{ivl} + \delta_{jvl}^{ivk})\epsilon_v, \end{aligned} \quad (2)$$

where ϵ_i is the strain, λ and μ are the Lamé elastic constants, and (l, m, n) the third order elastic constants derived by Murnaghan’s equation of state. Using Eq. (2) and the new value of δ_{ij} defined in Eq. (1), the interaction between the

conditioning and classical nonlinearity can be entirely described.

Following the experimental procedure used by Renaud *et al.*,⁶ but using three polarized waves, the four nonlinear parameters (l, m, n, α) are evaluated experimentally in a prismatic mortar sample with dimensions $28.5 \times 2.5 \times 2.5 \text{ cm}^3$. The Lamé elastic constants are determined experimentally via the measurements of the time of flight of compressional and shear waves: $\lambda = 18.5 \text{ GPa}$ and $\mu = 10 \text{ GPa}$. The position of the maximal strain amplitude is found by combining numerical simulations with experimental verification, according to the method proposed by Payan *et al.*¹⁷ This location was selected to position shear and compressional ultrasonic transducers. A short pulse centered at 1 MHz with a repetition rate of 2.5 kHz was used. Signals were recorded using a 12-bit Lecroy HDO 4024 oscilloscope at a 50 MHz sampling rate. As specified by Rivière *et al.*,⁷ the time of flight of each pulse needs to be less than a tenth of the period of the low-frequency excitation (pump), ensuring a quasi-constant strain during the travel of the ultrasonic probe wave. Seven amplitudes of low-frequency excitation were used and for each of them, the three velocity measurements are also performed three times, paying attention that the medium has fully recovered its undisturbed elastic properties between each test. Even though a steady-state regime is not reached during the experiment, it is assumed that the nonlinear behavior stabilizes after several cycles of the low-frequency excitation.⁷ In addition, the strain field is considered uniform on the entire high-frequency propagating zone. For the first longitudinal mode, the strain tensor is already diagonal and can be written as

$$\underline{\epsilon} = \begin{pmatrix} \epsilon & 0 & 0 \\ 0 & -\nu\epsilon & 0 \\ 0 & 0 & -\nu\epsilon \end{pmatrix}. \quad (3)$$

The Christoffel tensor $\Gamma_{il} = C_{ijkl}n_jn_k$ can be calculated using the strain field given by Eq. (3) and the elastic tensor given by Eq. (2). Through its diagonalization, the speed of sound for three polarized waves is obtained in any direction. Fig. 1 presents the “surface speed” obtained for longitudinal and shear (vertical and horizontal with respect to the geometric plan (2, 3)) waves. Under dynamic loading, the isotropic surface speed is contracted due to conditioning and oscillates with the instantaneous strain field $\underline{\epsilon}$ due to the classical nonlinear elasticity. On the “2” axis direction ($\theta = 0$), the wave speeds are expressed as

$$\begin{cases} \rho V_{22}^2 = C_{2222} = [(\lambda + \mu) + 2(l - \mu)Tr(\underline{\epsilon}) + 4(\lambda + m + \mu)\epsilon_2] \Lambda_{22}^2 & (4a) \\ \rho V_{21}^2 = C_{1212} = [\mu + (\lambda + m - \mu)Tr(\underline{\epsilon}) + 2\mu(\epsilon_1 + 2\epsilon_2)] \Lambda_{22}\Lambda_{11} - \frac{n}{2}\epsilon_3\Lambda_{11}\Lambda_{22}\Lambda_{33} & (4b) \\ \rho V_{23}^2 = C_{2323} = [\mu + (\lambda + m - \mu)Tr(\underline{\epsilon}) + 2\mu(\epsilon_2 + 2\epsilon_3)] \Lambda_{22}\Lambda_{33} - \frac{n}{2}\epsilon_1\Lambda_{11}\Lambda_{22}\Lambda_{33}. & (4c) \end{cases}$$

Terms in $\prod_{i,j}\Lambda_{ij}$ lead to quadratic and cubic effects of $(\alpha\Delta\epsilon)$. This product is relatively small for mortar ($10^{-3} - 10^{-4}$ with $\alpha \sim 100$ and $\Delta\epsilon \sim 10^{-6}$).¹⁷ $\Lambda_{ij}\Lambda_{kl}$ and $\Lambda_{ij}\Lambda_{kl}\Lambda_{mn}$ can then be

simplified to $\delta_{ij}\delta_{kl}(1 - \alpha(\Delta\epsilon_i + \Delta\epsilon_k))$ and $\delta_{ij}\delta_{kl}\delta_{mn}(1 - \alpha(\Delta\epsilon_i + \Delta\epsilon_k + \Delta\epsilon_m))$, respectively, in order to keep only linear dependencies with strain amplitudes. The elasticity

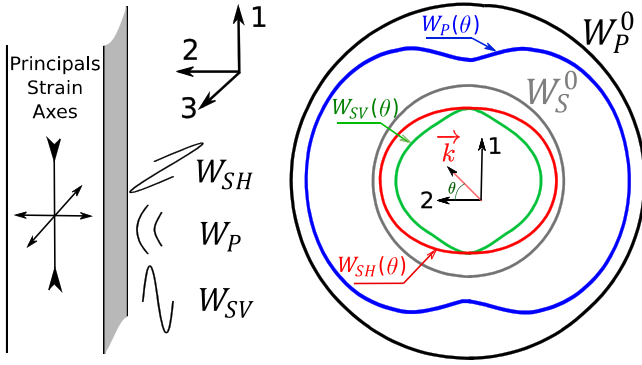


FIG. 1. “Surface Speed” computed analytically for the three polarized (pressure W_P , horizontal W_{SH} , and vertical W_{SV} shear) pulses used in the experiments as a function of the direction of propagation θ . Because of conditioning, the strain amplitude measured by the probe depends on the wave polarization and direction of propagation.

tensor now depends on the “instantaneous” strain ϵ and the strain amplitude $\Delta\epsilon$. This leads to the expression of the differential dC_{ijkl} as

$$dC_{ijkl} = \frac{\partial C_{ijkl}}{\partial \epsilon} d\epsilon + \frac{\partial C_{ijkl}}{\partial \Delta\epsilon} d\Delta\epsilon. \quad (5)$$

Under those assumptions, oscillations in the elastic modulus are proportional to a sinusoidal function. Then, the average over time of $d\epsilon$ being zero, the conditioning can be extracted as

$$\left\langle \frac{\Delta V_{2i}}{V_{2i}^0} \right\rangle_T = \frac{1}{2} \left\langle \frac{\Delta C_{2i2i}}{C_{2i2i}^0} \right\rangle_T.$$

Then

$$\left\{ \begin{array}{l} \left\langle \frac{\Delta V_{22}}{V_{22}} \right\rangle_T = -\alpha\nu\Delta\epsilon \\ \left\langle \frac{\Delta V_{21}}{V_{21}} \right\rangle_T = -\alpha \frac{(1+\nu)}{2} \Delta\epsilon \\ \left\langle \frac{\Delta V_{23}}{V_{23}} \right\rangle_T = -\alpha\nu\Delta\epsilon. \end{array} \right. \quad (6a)$$

(6a)

(6b)

(6c)

These expressions give redundant information which allows verifying the validity of the measurements. For each strain amplitude variation $\Delta\epsilon$, the relative change in velocity is evaluated. It is worth mentioning that the material is here under longitudinal dynamic loading and the principal strain axes match vectors of the geometric basis \vec{n}_i . A moving average window is applied to the relative wave speed shifting to remove the effect of the instantaneous strain. The values obtained for the three polarized pulses are shown in Fig. 2. A greater effect on the shear pulse W_{21} , polarized along the axis of maximum strain and a similar one on the shear W_{23} and longitudinal W_{22} pulses, polarized perpendicularly to the axis of maximum strain are well predicted by Eq. (6). The conditioning parameter is found to be consistent over the three polarization measurements with $\alpha = 85 \pm 10$. Murnaghan constants are then obtained by solving for the three unknowns in Eqs. (4a)–(4c). Velocity measurements highly depend on the strain and strain rate through the

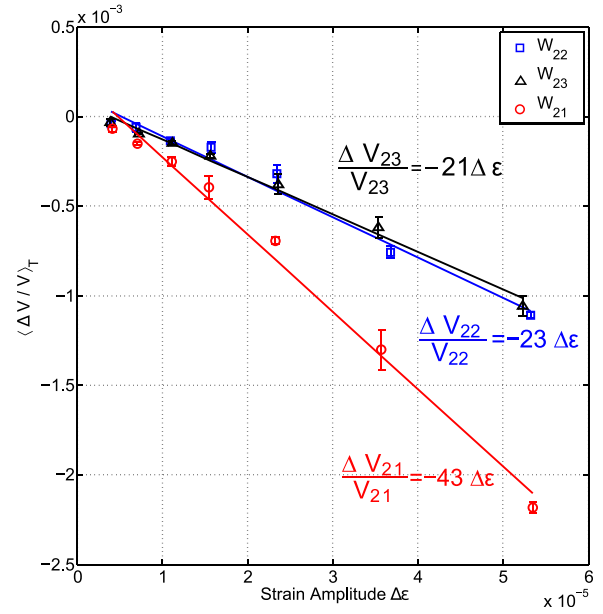


FIG. 2. Linear regression of $\langle \frac{\Delta V_{ij}}{V_{ij}} \rangle_T$ over strain amplitude $\Delta\epsilon$ for the three polarized (pressure W_{22} , horizontal W_{23} , and vertical W_{21} shear) waves propagating on the “2” axis direction. The slopes are linked to the conditioning based on Eq. (6).

nonlinear viscosity. Like in rocks, the attenuation of the probe pulse is different in compression or tension states. By dispersing the high-frequency pulses, dynamic strain oscillations should produce some hysteretic effects on the modulus measurements. Because the elastic model proposed in this letter is undamped, it is necessary to minimize the effects of strain induced attenuation when inverting Eqs. (4a)–(4c). Time of flight is obtained by cross-correlating emitted with transmitted signals. This measurement method may induce errors due to dissipative effects.¹⁸ With $ka < 1$ (k the wave number and a the characteristic length of a scatterer ranging from 50 to 200 μm) for the probe wave, this experiment is conducted in a Rayleigh diffusive regime. Considering the ballistic signals, the cross-correlation method gives an average of viscoelastic effects on the pulse bandwidth. Relative Amplitude Modulation (RAM: $\Delta A/A_0$) of the transmitted pulses for each polarization brings some helpful information to separate viscosity effects from purely elastic ones. RAM is calculated starting from the first transmitted pulse, before low frequency activation. Measured effects are then only produced by the strain field.¹⁹ Effects in the maximum compression zone are close to zero, as in most of the experimental data available in the literature in similar materials.^{6,7} Thus, at maximum compressive strain amplitude (negative values), the low frequency is perfectly in phase opposition with respect to the relative velocity changes. Consequently, to avoid viscoelastic effects on the measurement of the Murnaghan constants, Eqs. (4a)–(4c) are inverted at the compression maximum only. As shown in Fig. 3, the Murnaghan constants (l , m , n) are independent of the strain amplitude, thus demonstrating the validity of the model. The average values of (l , m , n) obtained herein are reported in Table I. These values are in good agreement with the previously reported values for concrete obtained using static acousto-elastic testing. Likewise, Murnaghan constants are negative in rocks, as measured by Winkler and Xingzhou.²⁰

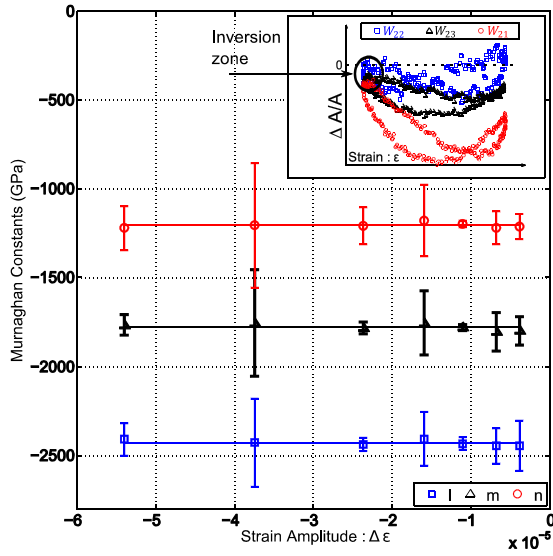


FIG. 3. Murnaghan coefficients estimated for seven excitation amplitudes in the mortar sample. Solid lines are the averaged values. Inset: RAM for the three polarized pulses at the highest amplitude of vibration. Eq. (4) is inverted in the maximum compression zone.

After the low frequency vibration completely vanishes, a relaxation process occurs in such a class of materials. TenCate *et al.*¹² suggest a logarithmic time dependency for the recovery of the Young modulus: $\Delta E/E_0 = m \log(t/t_0)$. They report a strain amplitude dependence of the slope “ m ” as in the present experiments (Fig. 4) using the three polarized waves. As for conditioning, one can observe an anisotropic effect with $m_{21} > m_{22} = m_{23}$. Using the anisotropic factor extracted from Eq. (1): $\langle \Delta V_{23}/\Delta V_{21} \rangle_T = 2\nu/(1 + \nu)$, the corrected values for W_{21} now match m_{22} and m_{23} . This result highlights the fact that for both conditioning and slow relaxation, the induced anisotropy is an isotropic effect related to the strain tensor, governed by a single scalar quantity.

In this letter, the three-dimensional nonlinear and nonequilibrium elasticity under dynamic loading is modeled using a tensorial approach and is validated experimentally. The effect of conditioning is uncoupled from the Murnaghan constants. It is shown that the higher order nonlinear elastic constants do not depend on the strain amplitude, unlike previous studies where experimental data are analyzed with a one-dimensional approximation.^{6,7} The values of the Murnaghan constants as well as conditioning reported in this study are in good agreement with the values reported for similar materials. The influence of viscoelasticity on the measurements is highlighted and a way to overcome it is proposed. It is also reported that despite apparent nonequilibrium anisotropy, both conditioning and slow dynamics are actually isotropic effects driven by the strain tensor through

TABLE I. Measured values of Murnaghan constants for comparison purposes, the values measured in concrete using static acousto-elasticity testing are also reported.⁴

(GPa)	l	m	n
Mortar	-2432	-1782	-1210
Concrete	-3007	-2283	-1813

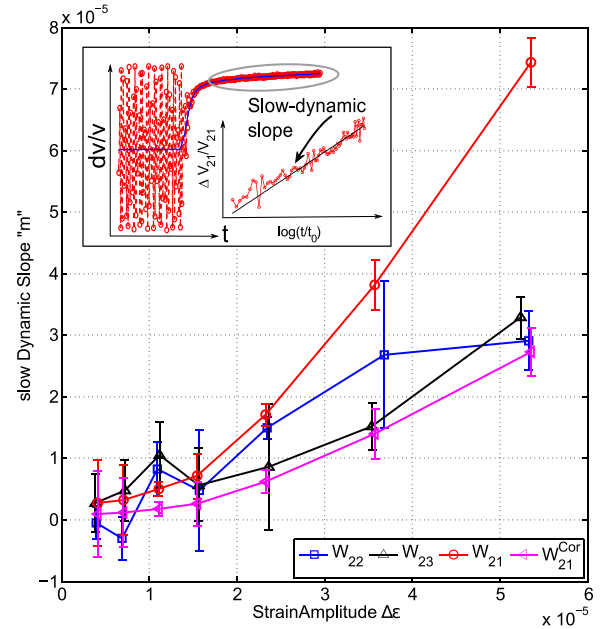


FIG. 4. Amplitude dependence of the slow dynamics slopes for the three polarized (pressure W_{22} , horizontal W_{23} , and vertical W_{21} shear) waves. The induced anisotropy is also present in the relaxation process. Inset: Calculation of the slow-dynamic slope.

scalar quantities α , l , m , and n . In the future, it would be interesting to extend the proposed tensorial description of nonequilibrium dynamics to any kind of dynamic loading (pump), so that the model applies to not only longitudinal modes but also torsional and bending modes of vibration. Such effort would be particularly important to explain the experimental results presented recently by Remillieux *et al.*²¹ on nonequilibrium dynamics measured globally on a sample excited by different types of modes. It would also be interesting to introduce nonlinear viscoelasticity in the present model, using an approach similar to that proposed by Favrie *et al.*²²

The authors acknowledge the support of the French National Research Agency through the ENDE program (Grant No. ANR-11 RSNR 0009).

¹F. D. Murnaghan, *Am. J. Math.* **59**, 235 (1937).

²D. S. Hughes and J. L. Kelly, *Phys. Rev.* **92**, 1145 (1953).

³D. M. Egle and D. E. Bray, *J. Acoust. Soc. Am.* **60**, 741 (1976).

⁴C. Payan, V. Garnier, J. Moysan, and P. A. Johnson, *Appl. Phys. Lett.* **94**, 011904 (2009).

⁵K. Winkler, A. Nur, and M. Gladwin, *Nature* **277**, 528 (1979).

⁶G. Renaud, J. Rivière, S. Hauptert, and P. Laugier, *J. Acoust. Soc. Am.* **133**, 3706 (2013).

⁷J. Rivière, G. Renaud, R. A. Guyer, and P. A. Johnson, *J. Appl. Phys.* **114**, 054905 (2013).

⁸R. A. Guyer and P. A. Johnson, *Phys. Today* **52**(4), 30 (1999).

⁹K. R. McCall and R. A. Guyer, *J. Geophys. Res.* **99**, 23887, doi:10.1029/94JB01941 (1994).

¹⁰P. Johnson and A. Sutin, *J. Acoust. Soc. Am.* **117**, 124 (2005).

¹¹V. Tournat, V. Zaitsev, V. Gusev, V. Nazarov, P. Béquin, and B. Castagnede, *Phys. Rev. Lett.* **92**, 085502 (2004).

¹²J. A. TenCate, E. Smith, and R. A. Guyer, *Phys. Rev. Lett.* **85**, 1020 (2000).

¹³O. O. Vakhnenko, V. V. Vakhnenko, T. J. Shankland, and J. A. TenCate, *Phys. Rev. E* **70**, 015602 (2004).

¹⁴V. Y. Zaitsev, V. E. Gusev, V. Tournat, and P. Richard, *Phys. Rev. Lett.* **112**, 108302 (2014).

- ¹⁵M. Nobili and M. Scalerandi, [Phys. Rev. B](#) **69**, 104105 (2004).
- ¹⁶L. Bocquet, E. Charlaix, S. Ciliberto, and J. Crassous, [Nature](#) **396**, 735 (1998).
- ¹⁷C. Payan, T. J. Ulrich, P. Y. Le Bas, T. Saleh, and M. Guimaraes, [J. Acoust. Soc. Am.](#) **136**, 537 (2014).
- ¹⁸G. Renaud, J. G. Bosch, A. F. W. van der Steen, and N. de Jong, [J. Acoust. Soc. Am.](#) **138**, 2668 (2015).
- ¹⁹C. Trarieux, S. Calle, H. Moreschi, G. Renaud, and M. Defontaine, [Appl. Phys. Lett.](#) **105**, 264103 (2014).
- ²⁰K. W. Winkler and X. Liu, [J. Acoust. Soc. Am.](#) **100**, 1392 (1996).
- ²¹M. C. Remillieux, R. A. Guyer, C. Payan, and T. J. Ulrich, [Phys. Rev. Lett.](#) **116**, 115501 (2016).
- ²²N. Favrie, B. Lombard, and C. Payan, [Wave Motion](#) **56**, 221 (2015).